Nonviral Vector-Based Gene Transfection of Primary Human Skeletal Myoblasts

Lei Ye,* Husnain Kh Haider,† Wahidah Bte Esa,* Peter K. Law,‡ Wei Zhang,§ LiPing Su,§ Yong Zhang,|| and Eugene K. W. Sim¶,[1]

*National University Medical Institutes, National University of Singapore, Singapore 117597; †Department of Pathology and Laboratory Medicine, College of Medicine, University of Cincinnati, Cincinnati, Ohio 45267; ‡Cell Transplants Singapore Pte. Ltd., Singapore 117684; §National Heart Center, Singapore 168752; ||Division of Bioengineering, Faculty of Engineering, National University of Singapore, Singapore 117574; and ¶Department of Surgery, Yong Loo Lin School of Medicine, National University of Singapore, Singapore 117597 and Gleneagles JPMC Cardiac Center, Brunei Darussalam BN2311

Low-level transgene efficiency is one of the main obstacles in *ex vivo* nonviral vector–mediated gene transfer into primary human skeletal myoblasts (hSkMs). We optimized the cholesterol:N-[1-(2, 3-dioleoyloxy)propyl]-N, N, N-trimethylammonium methylsulfate liposome (CD liposome) and 22-kDa polyethylenimine (PEI22)– and 25-kDa polyethylenimine (PEI25)–mediated transfection of primary hSkMs for angiogenic gene delivery. We found that transfection efficiency and cell viability of three nonviral vectors were cell passage dependent: early cell passages of hSkMs had higher transfection efficiencies with poor cell viabilities, whereas later cell passages of hSkMs had lower transfection efficiencies with better cell viabilities. Trypsinization improved the transfection efficiency by 20% to 60% compared with adherent hSkMs. Optimum gene transfection efficiency was found with passage 6 trypsinized hSkMs: transfection efficiency with CD lipoplexes was 6.99 ± 0.13%, PEI22 polyplexes was 18.58 ± 1.57%, and PEI25 polyplexes was 13.32 ± 0.88%. When pEGFP (a plasmid encoding the enhanced green fluorescent protein) was replaced with a vector containing human vascular endothelial growth factor 165 (phVEGF$_{165}$), the optimized gene transfection conditions resulted in hVEGF$_{165}$ expression up to Day 18 with a peak level at Day 2 after transfection. This study demonstrated that therapeutic angiogenic gene transfer through CD or PEI is feasible and safe after optimization. It could be a potential strategy for treatment of ischemic disease for angiomyogenesis. Exp Biol Med 232:1477–1487, 2007

Key words: angiogenesis; gene transfer; nonviral vector; skeletal myoblasts

Introduction

Skeletal myoblast (SkM) transplantation to regenerate functional muscle and therapeutic angiogenesis in post-infarction scar tissue have been well studied in experimental animal and clinical studies (1, 2). A more efficient approach will be the combined cell and angiogenic gene delivery for cardiac repair. The feasibility of SkM-mediated angiogenic gene transfer has shown better efficacy in the treatment of injured heart function (3, 4).

Cellular angiogenesis using genetically engineered SkMs has more advantages, such as localized transgene expression and reduced inflammation. SkMs as carriers of angiogenic genes hold great promise for treatment of ischemic heart disease; however, the approach of SkM transfection has not yet been optimized. Various viral vectors, including adenovirus, adeno-associated virus, and retrovirus, have been investigated (3–6). They have relatively high efficiency in transducing cells. However, problems such as high immunogenicity, tumorigenic potential, and inflammation inducement have limited the clinical application of viral vectors (7). So far human clinical studies have shown that the use of viral vectors causes inflammatory reactions, formation of antiadenoviral antibodies, transient fever, and increases in the presence of liver transaminase (8–10). In light of these concerns, there is a pressing need to develop a safer and more efficient nonviral gene delivery system that can circumvent the limitations of viral vectors. Among the variety of different

This project was funded by Singapore National Medical Research Council grant R-364-000-021–213.

[1] To whom correspondence should be addressed at Department of Surgery, National University of Singapore, 10 Medical Drive, Singapore 117597. E-mail: sursimkw@nus.edu.sg

Received June 30, 2007.
Accepted August 02, 2007.

DOI: 10.3181/0706-RM-175
1535-3702/07/23211-1477$15.00

materials that have been used in the development of nonviral vectors, cationic lipids and polymers have been found to confer several advantages such as ease of preparation, purification, and chemical modification, as well as stability (11, 12).

In the present study, three nonviral vectors were developed and compared for their gene transfection efficiency into primary human SkMs (hSkMs). A liposome based on cholesterol (Chol) + N-[1-(2, 3-dioleoyloxy)propyl]-N, N, N-trimethylammonium methylsulfate (DOTAP) (CD liposome) was developed as a cationic lipid vector. Polyethylenimine (PEI) of 22 kDa (PEI22) and 25 kDa (PEI25) was used for the development of cationic polymer vectors. The transfection efficiency of the three vectors was assessed by expressing the enhanced green fluorescent protein (pEGFP) gene in hSkMs. We found that the transfection efficiency of nonviral vectors was influenced by multiple factors. Based on the tested transfection conditions, the three nonviral vectors were further used as carriers of human vascular endothelial growth factor 165 plasmid ($phVEGF_{165}$) to transfect hSkMs.

Materials and Methods

Preparation of Liposomes and Lipoplexes with pEGFP. The CD liposome was prepared by mixing Chol (Sigma-Aldrich, St. Louis, MO) and DOTAP (Roche Pharma AG, Grenzach-Wyhlen, Germany) with ratios from 1:1 to 1:6 (w/w). The CD liposome and plasmid DNA were diluted in 30 μl and 70 μl, respectively, of sample buffer (20 m*M* HEPES in 150 m*M* NaCl [pH 7.4]) separately. The CD lipoplexes were developed based on the ratio (w/w) of CD liposome:pEGFP (4.7 kb; Clontech Laboratories, Inc., Mountain View, CA) by mixing the respective solutions containing CD liposome and plasmid DNA. After mixing, the mixture was pipetted for 30 secs followed by an incubation for 30 mins at 37°C. Then the CD lipoplex mixture was added to cell culture medium (10% Dulbecco modified Eagle medium [DMEM]) for transfection into hSkMs for 24 hrs at 37°C in an incubator.

Preparation of PEI and Polyplexes with pEGFP. PEI22 (5.47 m*M*) was purchased from Euromedex (Souffelweyersheim, France), and PEI25 was purchased from Sigma-Aldrich. PEI was diluted in distilled water to 10 m*M* and passed through a 0.22-μm filter. Plasmid DNA and PEI25 or PEI22 were diluted in 50 μl of 150 m*M* NaCl separately. Polyplexes were developed by mixing the respective NaCl solutions containing PEI or plasmid DNA. After complexation, the mixtures were vortexed for 30 sec followed by incubation for 10 min. Then the polyplex mixtures were added into culture medium for transfection with hSkMs for 24 hrs at 37°C in an incubator. The PEI:DNA ratio was based on the equivalents of PEI nitrogen per DNA phosphate (N/P). The N/P ratio was calculated using the following equation:

$$N/P = V/(Q_{DNA} \times 3)$$

for which V = volume (μl) of 10m*M* PEI25 or 5.47 m*M* PEI22 and Q_{DNA} = quantity of DNA (μg) used per 1×10^5 hSkMs.

Particle Size and Zeta Potential Analysis. The sizes of the lipoplexes and polyplexes were measured by dynamic light scattering. Together with the size distribution, zeta potential was determined with a Zetasizer Nano-ZS (Malvern Instruments, Worcestershire, UK) equipped with a 4-mW, 633-nm Ne-He laser at 25°C and a fixed scattering angle of 90 degrees. The measurement of zeta potential was performed in distilled water instead of high ionic–strength buffer because of the electrophoretic immobility of relatively large lipoplexes and polyplexes due to an excess of ions.

Scanning Electron Microscopy. Scanning electron microscopy was used to image the shapes and sizes of lipoplexes and polyplexes. The buffers containing the polyplexes were spread on specimen stub (Agar Scientific Ltd., Essex, UK) and air-dried. The lipoplexes were first fixed in 2.5% glutaraldehyde for 4 hrs at room temperature followed by 1% osmium tetroxide fixation at pH 7.4 for 1 hr. The samples were placed onto poly-L-lysine–coated coverslips and air-dried. After washing in deionized H_2O for 10 mins, the samples were dehydrated in an ethanol series (25%–100%) at room temperature and placed on specimen stubs. Air-dried polyplex and lipoplex samples were coated with gold at a current of 30 mA for 30 secs using the SCD005 Sputter Coater (BAL-TEC AG, Balzers, Liechtenstein) and viewed under the XL30 FEG Philips electron microscopy (FEI Comp., Hillsboro, OR).

Loading Efficiency of Lipoplex and Polyplex Particles. The amount of encapsulated DNA in the lipoplexes and polyplexes was calculated by measuring the difference between the amount of plasmid DNA added to the nanoparticle solution and the measured nonentrapped DNA remaining in the aqueous phase after particle formation. After complexation, the particle suspension was centrifuged for 15 mins at 8000 rpm at room temperature and the supernatant was checked for the nonbound DNA concentration with the NanoDrop ND-1000 spectrophotometer (Wilmington, DE).

Protection and Release Assay of DNA. For protection and release of DNA from the complexes, 50 μl of 10X DNase buffer (Promega Corp., Madison, WI) was mixed with 450 μl of solutions containing 10 μg of naked pEGFP, lipoplexes, or polyplexes carrying pEGFP: CD-pEGFP, PEI22-pEGFP, and PEI25-pEGFP. After 100 μl was withdrawn at Time 0, 2 units of DNase I (Promega) was added to the mixture, which was then incubated at 37°C. Sample solution (100 μl) was sampled at 0.5, 1, 1.5, and 2 hrs after incubation for analysis. To inactivate DNase I, all samples were treated with 10 μl of EDTA (20 m*M*) for 10 mins at 65°C. Finally, 10 μl of 10% sodium dodecyl sulfate was added into the lipoplex buffer, and the mixture was incubated for 2 hrs at 65°C. Ten microliters of heparin (5 IU/μl; Mayne Pharma, Melbourne, Australia) was added

into the polyplex buffer, and the mixture was incubated overnight to facilitate dissociation of pEGFP. The final samples were electrophoresed using a 1% agarose gel for analysis on the Gel Document System (Bio-Rad, Hercules, CA).

Culture of hSkMs. Primary hSkMs were purchased from Bioheart, Inc. (Sunrise, FL). The cells were cultured and propagated in 225-mm^2 tissue culture flasks using Super medium (kindly provided by Cell Transplants Singapore Pte Ltd, Singapore) supplemented with 10% fetal calf serum and antibiotics at 37°C in a 5% CO_2 incubator until confluent. The purity and uniformity of the hSkM culture were assessed by desmin and CD56 expression. The cells were fixed in −20°C methanol for 10 mins followed by incubation with 0.1% Triton X-100 for another 10 mins. After blocking with ultra-U block (Lab Vision Products, Fremont, CA) for 8 mins, 1:50 dilutions of rabbit anti-desmin antibody (Sigma-Aldrich) and mouse anti–human CD56-phycoerythrin (PE) antibody (BD PharMingen, San Diego, CA) were added onto the samples. After a 1-hr incubation, cells were washed and incubated with a 1:200 dilution of goat anti-rabbit IgG-fluorescein isothiocyanate (FITC) (Sigma-Aldrich) for 1 hr at room temperature for detection of desmin. The samples were washed and observed under a fluorescent microscope (IX70; Olympus, Tokyo, Japan).

Transfection of hSkMs. Adherent and trypsinized hSkMs at passage 4 (P4), passage 6 (P6), and passage 9 (P9) were used at a density of 1×10^5 cells per well in a 12-well plate. Each experiment was repeated thrice.

Transfection of hSkMs Using Lipoplexes. Ratios (w/w) of 1:1 to 1:6 of Chol:DOTAP were complexed with 2 μg of pEGFP. Based on the optimal ratio between Chol and DOTAP, the ratio (w/w) between the CD liposome and pEGFP (2 μg) was increased from 3:1 to 18:1. Similarly, the amount of pEGFP DNA was increased from 2 μg to 5 μg using the optimal ratio between CD liposome and pEGFP. The CD lipoplexes were developed as described above and added into culture medium for transfection with adherent or trypsinized hSkMs for 24 hrs at 37°C in an incubator.

Transfection of hSkMs Using Polyplexes. The polyplexes were formed based on the N/P ratio. For PEI22, the N/P ratio was tested from 3:1 to 18:1, whereas the N/P ratio was tested from 9:1 to 24:1 for PEI25. Next pEGFP DNA was increased from 2 μg to 5 μg using the optimal N/P ratio. The polyplexes were developed as described above and added into culture medium to transfect adherent or trypsinized hSkMs for 24 hrs at 37°C.

The transfection medium was removed, and the cells were washed with phosphate-buffered saline and fresh DMEM containing 10% fetal bovine serum. The transfected hSkMs were assessed for gene transfection efficiency and cell viability.

Transfection Efficiency and Cell Viability. Transfection efficiency and cell viability of hSkMs were analyzed using an Epics Elite Esp flow cytometer (Beckman Coulter, Fullerton, CA). Cells with adequate size and granularity were included in the statistical analysis (13). Nontransfected and CD liposome–, PEI22-, and PEI25-transfected hSkMs were used for baseline settings of the autofluorescence limit. Data were analyzed using WinMDI version 2.8 (Scripps Research Institute, La Jolla, CA) with gating at 1%.

Transfection of hSkMs with CD-phVEGF$_{165}$ or PEI-phVEGF$_{165}$. The pCI plasmid with a CMV promoter was purchased from Promega. A fragment of 750 bp containing hVEGF$_{165}$ was ligated into the pCI vector to create phVEGF$_{165}$ (4.75 kb).hSkMs were transfected with lipoplexes or polyplexes carrying phVEGF$_{165}$ using the optimized transfection conditions based on flow cytometry results. The hVEGF$_{165}$ gene expression efficiency was analyzed by immunostaining, quantitative reverse transcription polymerase chain reaction (QRT-PCR), and enzyme linked immunosorbent assay (ELISA).

Immunohistochemical Staining. The transfected cells were grown in chambered slides for 24 hrs. After fixation in 50% methanol/acetone, the cells were incubated with 0.1% Triton X-100, followed by blocking for 8 mins with ultra-U block (Lab Vision Products). The cells were incubated at 37°C with a 1:200 dilution of rabbit anti-VEGF$_{165}$ primary antibody (Chemicon International Inc., Temecula, CA) for 24 hrs. Expression of VEGF was detected by the addition of goat anti-rabbit-IgG conjugated with tetramethylrhodamine isothiocyanate (Sigma-Aldrich) for 1 hr and visualized under fluorescent microscopy (Olympus).

QRT-PCR Analysis for hVEGF$_{165}$ Gene Expression. Nontransfected, CD-phVEGF$_{165}$–, and PEI-phVEGF$_{165}$–transfected hSkM samples from 2, 4, 8, and 18 days after transfection were collected to quantify hVEGF$_{165}$ expression. The following primers were used to analyze hVEGF$_{165}$ expression (303 bp):

1. Sense: 5′-ATG AAC TTT CTG CTG TCT TGG-3′
2. Antisense: 5′-GTT GGA CTC CTC AGT GGG C-3′
3. 18S rRNA (Ambion, Inc., Austin, TX) was amplified as an internal control.

Total RNA was isolated using a total RNA isolation kit (QIAGEN, Hilden, Germany) as per the supplier's instructions. Total RNA (250 ng) was treated with DNase I (Promega) to remove DNA contamination. RNA was reverse transcribed to cDNA, and expression of hVEGF$_{165}$ was quantified using the ABsolute MAX 2-Step QRT-PCR SYBR Green Kit (ABgene, Epsom, UK) as per the supplier's instructions. Briefly, RNA template, oligo(dT), dNTPs, 5X first-strand synthesis buffer, and ABsolute MAX QRTase were mixed and incubated at 42°C for 60 mins, followed by an incubation for 10 mins at 75°C to inactivate ABsolute MAX QRTase. The amplification mixture was prepared by mixing ABsolute QPCR SYBR Green Mix, hVEGF$_{165}$ primers, and reverse transcription cDNA buffer. The QPCR thermal cycler was programmed as follows: 1

Table 1. Average Particle Size and Zeta Potential of (A) CD-pEGFP Lipoplexes, (B) PEI22-pEGFP Polyplexes, and (C) PEI25-pEGFP Polyplexes

A				
CD liposome:DNA	6:1	9:1	12:1	15:1
Particle size (nm)	86.62 ± 2.14	96.71 ± 4.31	103.2 ± 2.9	139.39 ± 8.86
Zeta potential (mV)	41.93 ± 0.15	42.17 ± 1.23	45.97 ± 1.02	48.83 ± 1.64
B				
N/P ratio	6:1	9:1	12:1	15:1
Particle size (nm)	73.58 ± 2.47	76.90 ± 6.62	92.54 ± 11.13	96.78 ± 12.58
Zeta potential (mV)	20.15 ± 0.45	26.17 ± 1.3	26.58 ± 2.07	28.03 ± 3.18
C				
N/P ratio	15:1	18:1	21:1	24:1
Particle size (nm)	87.75 ± 4.41	91.14 ± 3.14	101.31 ± 2.17	133.22 ± 6.85
Zeta potential (mV)	29.05 ± 1.06	34.62 ± 2.96	36.42 ± 1.15	39.88 ± 1.64

cycle at 95°C for 15 mins; denaturation at 95°C for 30 secs; annealing at 58°C for 30 secs; and extension at 72°C for 30 secs. A total of 40 cycles was performed. $hVEGF_{165}$ expression after transfection was compared with non-transfected hSkMs and normalized with the expression of 18S rRNA.

ELISA for $hVEGF_{165}$. Transfected hSkMs (1×10^5) were grown in a 12-well plate, and the cell supernatant samples were collected at regular time intervals from Day 2 to Day 18 with 2-day intervals between samples. The samples were kept frozen at –20°C until use. For quantification of $hVEGF_{165}$, a VEGF sandwich ELISA kit (Chemicon International) was used according to the supplier's instructions (4).

Statistic Analysis. Statistical analysis was performed using SPSS (version 10.0; SPSS Inc., Chicago, IL). All data are presented as means ± SEM.

Results

Characterization of Lipoplex and Polyplex Particles. The average particle size and zeta potential showed concentration dependence with larger particle size and higher zeta potential at higher lipid or PEI:DNA ratio (Table 1). The average particle size of CD lipoplexes ranged from 86.62 ± 2.14 nm to 139.39 ± 8.86 nm, and zeta potential increased from 41.93 ± 0.15 mV to 48.83 ± 1.64 mV when the CD liposome:pEGFP ratio was between 6:1 and 15:1 (Table 1A). The average particle size of PEI22 polyplexes was between 73.58 ± 2.47 nm and 96.78 ± 12.58 nm, and the zeta potential accordingly increased from 20.15 ± 0.45 mV to 28.03 ± 3.18 mV at an N/P ratio between 6:1 and 15:1 (Table 1B). The average particle size of PEI25 polyplexes ranged from 87.75 ± 4.41 to 133.22 ± 6.85 nm, and the zeta potential increased from 29.05 ± 1.06 mV to 39.88 ± 1.64 mV when the N/P ratio was from 15:1 to 24:1 (Table 1C).

Most of the CD lipoplexes were microspheres with diameters ranging from 70 to 115 nm when the CD:DNA ratio was 12:1 (Fig. 1A). They were smaller than those (103.2 ± 2.9 nm) determined by the Zetasizer Nano ZS machine. PEI22 polyplexes were oval or spindle shaped when the N/P ratio was 9:1 (Fig. 1B). Their short-axis diameters were approximately 60 to 95 nm, whereas the long-axis diameters were approximately 80 to 130 nm. PEI25 polyplexes were either microspheres or spindle shaped with diameters between 60 and 180 nm when the N/P ratio was 21:1 (Fig. 1C).

Loading efficiency of the CD-DNA and PEI-DNA complexes was approximately 99%. A DNase I protection assay confirmed that CD, PEI22, and PEI25 protected the encapsulated DNA from degradation by DNase I for more than 2 hrs of observation, whereas the unprotected naked DNA was completely degraded by DNase I after 30 mins of incubation (Fig. 2).

Purity of hSkM Culture. The hSkM culture was more than 95% pure and simultaneously expressed desmin and CD56 (Fig. 3).

Transfection of hSkMs With CD-pEGFP. Although the highest transfection efficiency was achieved when the Chol:DOTAP ratio was 1:6 (0.9% ± 0.59%), it was marred by poor cell viability (76% ± 12.11%) (Fig. 4A). Thus, the Chol:DOTAP ratio at 1:4 (efficiency = 0.53% ± 0.18%; viability = 94% ± 5.54%) was chosen after balancing transfection efficiency and cell viability. Similarly, the CD:pEGFP (w/w) ratio was increased from 3:1 to 18:1 for P4, P6, and P9 adherent or trypsinized hSkMs with the Chol:DOTAP ratio at 1:4. It was at 12:1 CD:pEGFP that the highest transfection efficiency was achieved for P4 (6.91% ± 0.25%), P6 (3.09% ± 0.44%), and P9 (1.43% ± 0.04%) adherent hSkMs (Fig. 4B) and P4 (11.74% ± 1.29%) and P6 (6.1% ± 0.6%) trypsinized hSkMs (Fig. 4C). Furthermore, the amount of pEGFP was increased from 2 μg to 5 μg for trypsinized hSkMs with the CD:pEGFP ratio at 12:1. A further increase in transfection efficiency was achieved for P6 (6.99% ± 0.13%) and P9 (4.69% ± 0.55%) trypsinized hSkMs (Fig. 4D), whereas transfection efficiency was reduced to 8.55% ± 0.19% for P4 trypsinized hSkMs when the amount of pEGFP was increased to 3 μg. Although maximal gene transfection efficiency was

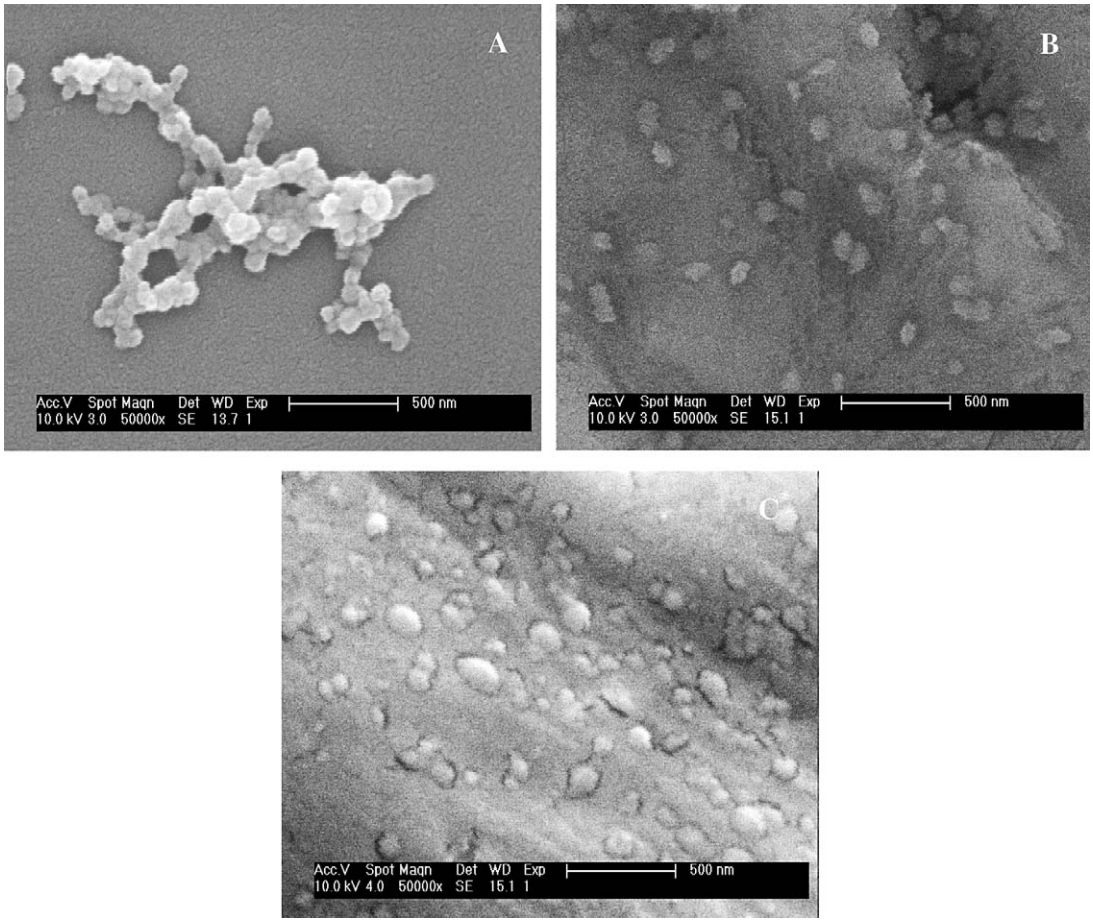

Figure 1. Scanning electron microscopy of (A) CD lipoplexes when the CD:pEGFP ratio was 12:1, (B) PEI22 polyplexes when the N/P ratio was 9:1, and (C) PEI25 polyplexes when the N/P ratio was 21:1. Bar, 500 nm.

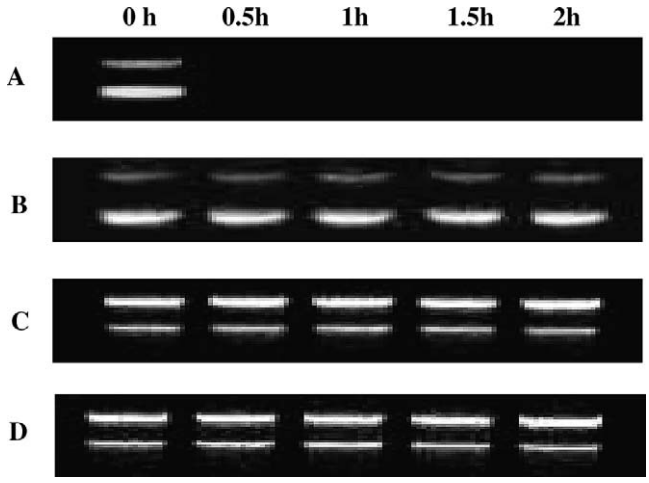

Figure 2. DNase I protection assay. Complexation of CD or PEI with DNA imparted stability to the encapsulated DNA against DNase I. (A) Naked plasmid DNA was totally degraded in the presence of DNase I after 0.5-h incubation. (B) CD-pEGFP, (C) PEI25-pEGFP, and (D) PEI22-pEGFP complexes protected pEGFP from degradation up to 2 hr in the presence of DNase I.

achieved for P4 trypsinized hSkMs when 2 μg of plasmid DNA was used per 1×10^5 cells, the accompanying poor cell viability rate (66.63% ± 3.18%) made it unfavorable for cell therapy. Thus, the optimal transfection conditions were a CD:DNA ratio of 12:1 with 3 μg of plasmid DNA per 1×10^5 P6 trypsinized hSkMs. Typical pictures of EGFP expression from CD-pEGFP–transfected trypsinized hSkMs at P4, P6, and P9 with a CD pEGFP ratio at 12:1 with 3 μg of pEGFP per 1×10^5 cells are shown in Figure 4E–G.

Transfection of hSkMs with PEI22-pEGFP. The N/P ratio of PEI22:pEGFP was first increased from 3:1 to 18:1 for P4, P6, and P9 adherent or trypsinized hSkMs (Fig. 5). It was at an N/P ratio of 9:1 that the highest transfection efficiency was achieved for P4, P6, and P9 adherent or trypsinized hSkMs (Fig. 5A and B). Trypsinization increased the transfection efficiency to 21.74% ± 0.94%, 18.58% ± 1.57%, and 6.63% ± 0.84% for P4, P6, and P9, respectively, compared with adherent hSkMs (17.58 ± 2.15%, 13.48 ± 0.2%, and 7.65 ± 0.78%, respectively). Next the amount of pEGFP was increased from 2 μg to 5 μg with the N/P ratio at 9:1 for trypsinized hSkMs. The increased DNA quantity did not further improve transfection

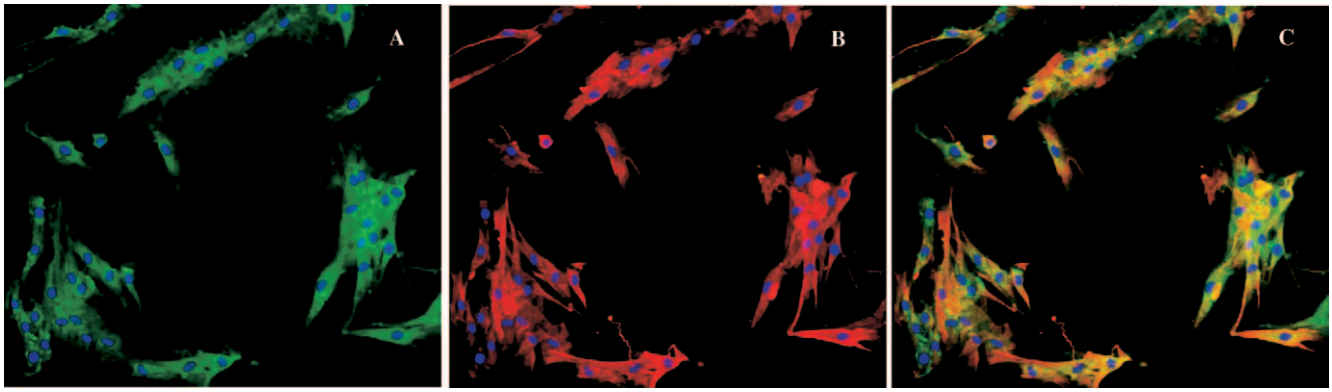

Figure 3. Dual fluorescent immunostaining of hSkMs for desmin and CD56 expression. (A) Desmin expression (green fluorescence = FITC).

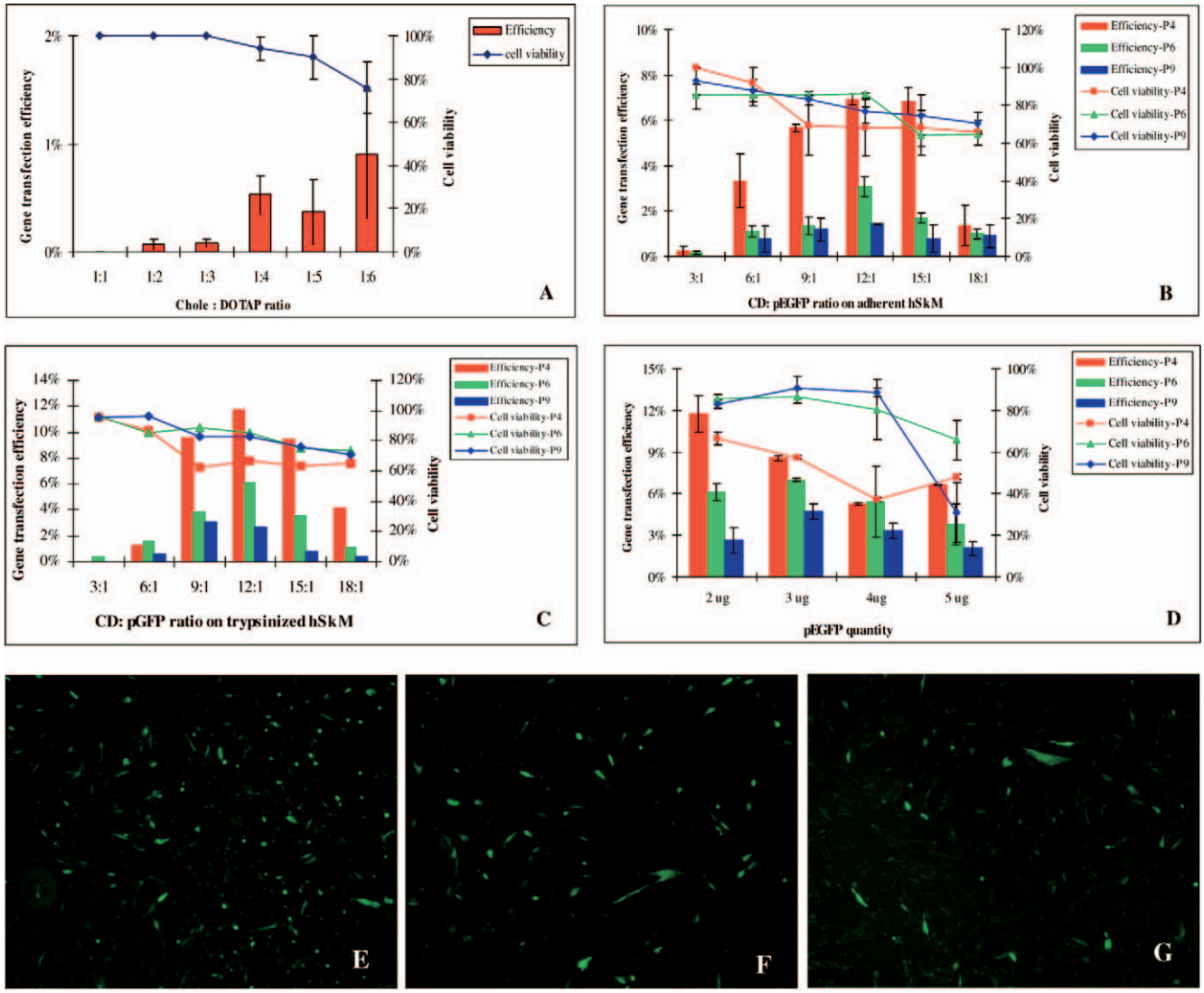

Figure 4. Optimization of CD-pEGFP transfection with hSkMs on P4, P6, and P9. (A) Gene transfection efficiency on P4 adherent hSkMs when the Chol:DOTAP ratio was increased from 1:1 to 1:6. (B) Gene transfection efficiency on adherent hSkMs when the CD:pEGFP ratio was increased from 3:1 to 18:1 with the Chol:DOTAP ratio at 1:4. (C) Gene transfection efficiency on trypsinized hSkMs when the CD:pEGFP ratio was increased from 3:1 to 18:1 with the Chol:DOTAP ratio at 1:4. (D) Gene transfection efficiency when the amount of pEGFP was increased from 2 μg to 5 μg with the CD:pEGFP ratio at 12:1. Typical pictures of pEGFP expression from CD-pEGFP–transfected trypsinized hSkMs at (E) P4, (F) P6, and (G) P9 with the CD:pEGFP ratio at 12:1 using 3 μg of pEGFP per 1×10^5 cells. Magnification: ×40. Color figure is available in the online version of the journal.

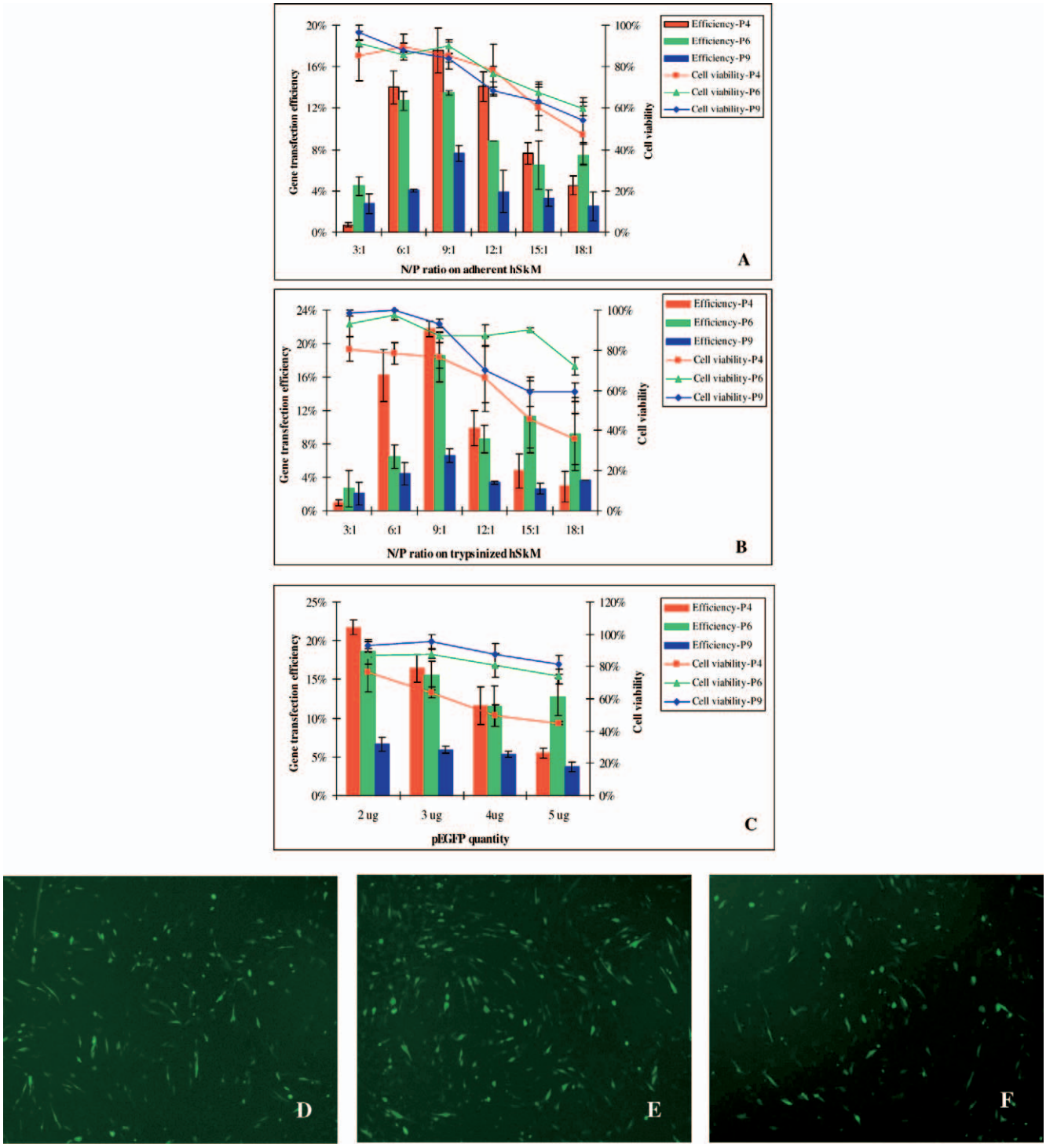

Figure 5. Optimization of PEI22-pEGFP transfection with hSkM on P4, P6, and P9. (A) Gene transfection efficiency on adherent hSkM when the N/P ratio was increased from 3:1 to 18:1. (B) Gene transfection efficiency on trypsinized hSkM when the N/P ratio was increased from 3:1 to 18:1. (C) Gene transfection efficiency when the amount of pEGFP was increased from 2 μg to 5 μg with the N/P ratio at 12:1. Typical pEGFP expression pictures of PEI22-pEGFP–transfected trypsinized hSkM at (D) P4, (E) P6, and (F) P9 when the N/P ratio was 9:1 using 2 μg of pEGFP per 1×10^5 cells. Magnification: ×40. Color figure is available in the online version of the journal.

efficiency; the highest transfection efficiency was still achieved at 2 μg of pEGFP when the N/P ratio was 9:1 on trypsinized hSkMs (Fig. 5C). Although the maximal gene transfection efficiency (21.74% ± 0.94%) was achieved for P4 trypsinized hSkMs with 2 μg of DNA per 1×10^5 cells with the N/P ratio at 9:1, the poor cell viability rate (76.63% ± 12.5%) made it unfavorable for gene transfection. Thus, after balancing the transfection efficiency

and cell viability, the optimal transfection condition chosen was an N/P ratio of 9:1 with plasmid DNA at 2 μg per 1×10^5 P6 trypsinized hSkMs. Typical EGFP expression of PEI22-pEGFP–transfected trypsinized hSkMs at P4, P6, and P9 when the N/P ratio was 9:1 using 2 μg of pEGFP per 1×10^5 cells is shown in Figure 5D–F.

Transfection of hSkMs With PEI25-pEGFP. The N/P ratio of EI25:pEGFP was first increased from 9:1 to 24:1 on P4, P6, and P9 adherent or trypsinized hSkMs. It was at an N/P ratio of 21:1 that the highest transfection efficiency was achieved using P4, P6, and P9 adherent or trypsinized hSkMs (Fig. 6A and B). Trypsinization increased the transfection efficiency to 10.15% ± 1.0%, 11.96% ± 3.7%, and 5.85% ± 1.51%, respectively, of the trypsinized hSkMs compared with the adherent hSkMs (8.96% ± 0.96%, 4.95% ± 1.56%, and 2.54% ± 0.4%, respectively). The increase in DNA quantity further improved the transfection efficiency. The highest transfection efficiency was achieved at 3 μg of pEGFP when the N/P ratio was 21:1 on trypsinized hSkMs (P4 = 10.21% ± 0.35%; P6 = 13.32% ± 0.88%; and P9 = 8.07% ± 0.74%) (Fig. 6C). Thus, considering the transfection efficiency and cell viability, the optimal transfection conditions were chosen as an N/P ratio of 21:1 with plasmid DNA at 3 μg per 1×10^5 P6 trypsinized hSkMs. Typical EGFP expression of PEI25-pEGFP–transfected trypsinized hSkMs at P4, P6, and P9 when the N/P ratio was at 21:1 using 3 μg of pEGFP per 1×10^5 cells is shown in Figure 6D–F.

Characterization of CD-phVEGF$_{165}$– and PEI-phVEGF$_{165}$–Transfected hSkMs. Replacing pEGFP with phVEGF$_{165}$, trypsinized hSkMs at P6 were transfected with CD-phVEGF$_{165}$, PEI22-phVEGF$_{165}$, and PEI25-phVEGF$_{165}$ using the aforementioned optimal transfection conditions. Immunohistochemical staining of hSkMs transfected with the three vectors revealed that the transfected hSkMs actively expressed hVEGF$_{165}$ (Fig. 7).

The presence of mRNA encoding hVEGF$_{165}$ as detected by hVEFG$_{165}$-specific primers revealed that phVEGF$_{165}$ transfection with hSkMs resulted in poor transfection efficiency (increased 0.32 ± 0.06 times compared with nontransfected hSkMs) (Fig. 8), whereas the CD-phVEGF$_{165}$, PEI22-phVEFG$_{165}$, and PEI25-phVEGF$_{165}$ transfections with hSkMs increased hVEGF$_{165}$ expression by 6.29 ± 0.24, 10.3 ± 0.54, and 8.37 ± 0.21 times, respectively, on Day 2; 5.94 ± 0.1, 8.68 ± 0.35, and 7.72 ± 0.27 times on Day 4; 1.43 ± 0.37, 3.26 ± 0.44, and 2.84 ± 0.29 times on Day 8; and 0.36 ± 0.27, 2.29 ± 0.94, and 1.69 ± 0.04 times on Day 18.

An ELISA for hVEGF$_{165}$ quantification was carried out using the supernatant from transfected hSkMs. The hSkMs transfected with CD-phVEGF$_{165}$, PEI22-phVEFG$_{165}$, and PEI25-phVEGF$_{165}$ were able to continuously secrete hVEGF$_{165}$ for at least 18 days *in vitro* (0.83 ± 0.08 ng/ml, 2.7 ± 0.6 ng/ml, and 1.17 ± 0.09 ng/ml, respectively), reaching peak expression on Day 2 after transfection (8.95 ± 0.55 ng/ml, 13.2 ± 1.2 ng/ml, and 10.8 ± 0.3 ng/ml, respectively) (Fig. 9), whereas the nontransfected hSKMs secreted low levels of VEGF$_{165}$ (300 ± 50 pg/ml) (3). The highest expression level was achieved by phVEGF$_{165}$ transfection mediated by PEI22.

Discussion

SkMs have been genetically modified to achieve overexpression of therapeutic proteins and growth factors. The angiogenic growth factors secreted by the genetically modified SkMs stimulate the growth of collateral vessels, producing a bio-bypass effect (3, 4). Currently, the *ex vivo* delivery of angiogenic genes into SkMs is mainly through viral vectors and naked DNA. Viral vectors have serious safety risks based upon their immunogenic nature and oncogenic potential (7). The delivery of naked plasmid DNA remains an inefficient gene transfer option. In this study, we showed the effectiveness of CD liposome– and PEI polymer–based nonviral vectors for gene transfection of primary hSkMs. Our results showed that gene transfer efficiency into primary hSkMs was cell passage dependent: the earlier passage cells were easy to transfect but showed poor cell viability. Furthermore, trypsinization improved the efficiency of transfection with any of the three nonviral vectors used in our study.

One noteworthy finding of the current study was that efficiency of the nonviral gene transfer was related to the cell passage number of primary hSkMs. The higher transfection efficiency in the earliest cell passage can be related to cell proliferation because more primary hSkMs are proliferating at earlier passages. It has been shown that CD lipoplexes and PEI25 and PEI22 polyplexes rely on the translocation of plasmid DNA into the nucleus predominantly during the S/G_2 phase of the cell cycle (14, 15). PEI22 polyplexes can also translocate pDNA into the nucleus independent of the cell cycle (12). Thus, the highest gene transfection efficiency was anticipated at P4, which incidentally had the highest rate of cell division. However, the P4 hSkMs were vulnerable to the toxicity of the CD lipid and PEI, making it an unsuitable stage for therapeutic gene transfer. We found that relatively high transfection efficiency with ideal cell viability could be achieved by P6 hSkMs. Our results clearly depict the significance of cell

→

Figure 6. Optimization of PEI25-pEGFP transfection with hSkM on P4, P6, and P9. (A) Gene transfection efficiency on adherent hSkM when the N/P ratio was increased from 9:1 to 24:1. (B) Gene transfection efficiency on trypsinized hSkM when the N/P ratio was increased from 9:1 to 24:1. (C) Gene transfection efficiency when the amount of pEGFP was increased from 2 μg to 5 μg with the N/P ratio at 21:1. Typical pEGFP expression pictures of PEI25-pEGFP–transfected trypsinized hSkM at (D) P4, (E) P6, and (F) P9 when the N/P ratio was 21:1 using 3 μg of pEGFP per 1×10^5 cells. Magnification: ×40. Color figure is available in the online version of the journal.

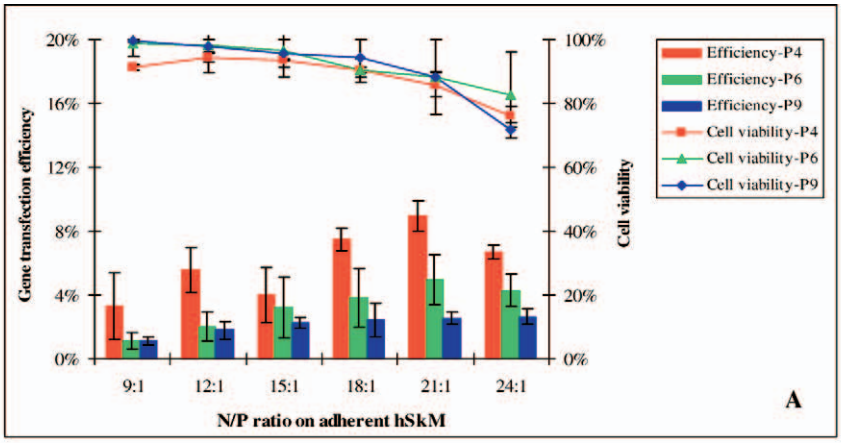

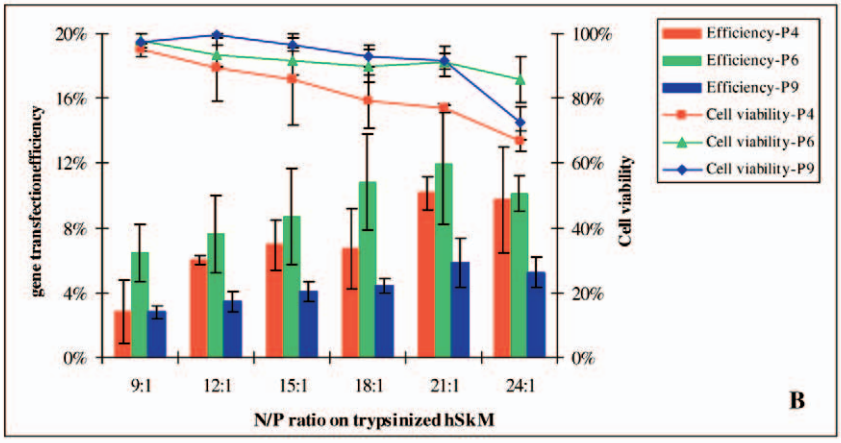

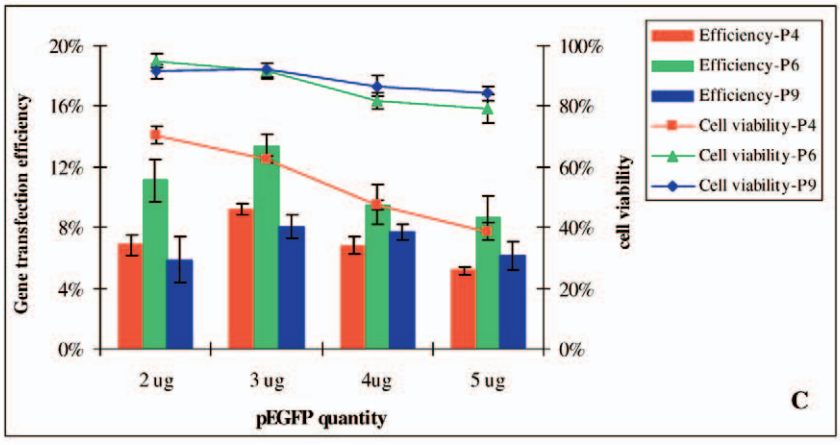

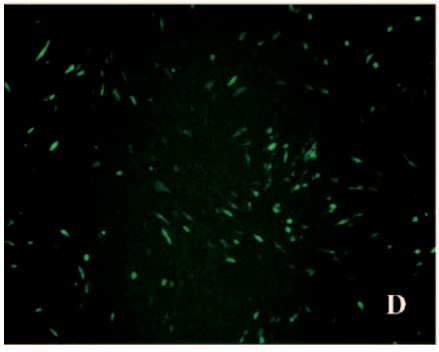

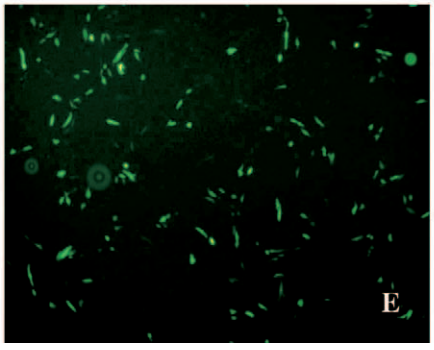

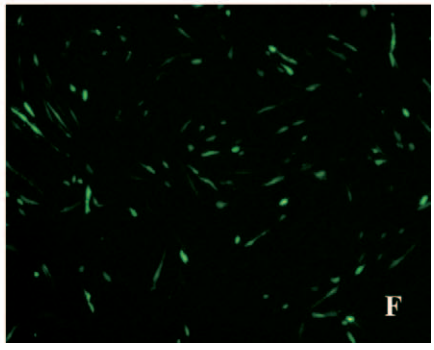

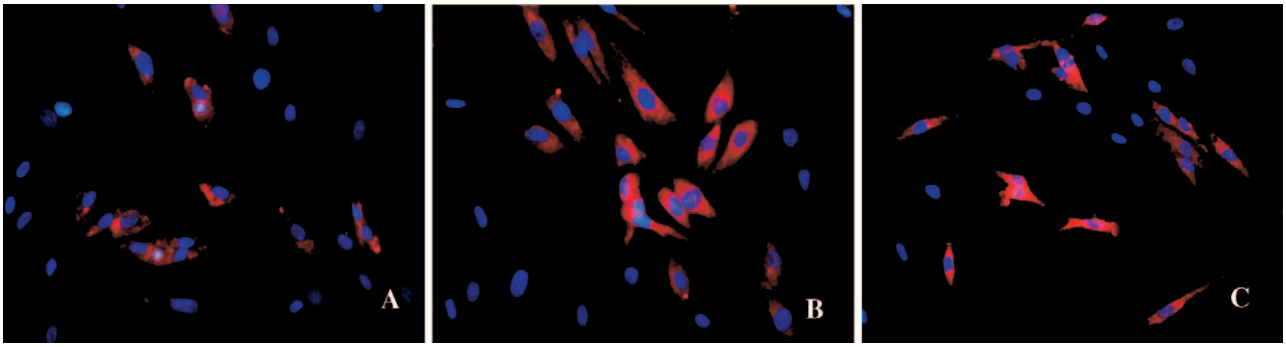

Figure 7. Immunostaining of hSkM for $hVEGF_{165}$ expression after transfection with (A) CD-$phVEGF_{165}$, (B) PEI22-$phVEGF_{165}$, and (C) PEI25-$phVEGF_{165}$. Magnification: ×200. Color figure is available in the online version of the journal.

passage number as an important factor when nonviral-mediated gene transfection is carried out on primary hSkMs. We found that trypsinization also improved CD- and PEI-mediated gene transfection efficiency at the three passages studied. This physical procedure improved transfection efficiency by 20% to 60%. Further study is needed to clarify the mechanism by which trypsin pretreatment enhanced the efficiency of nonviral vector–mediated gene therapy.

It is well known that low transfection efficiency is one of the big obstacles to *ex vivo* nonviral vector–mediated gene delivery into primary hSkMs. The gene transfection expression efficiencies of nonviral vector–mediated gene transfer are influenced by plasmid DNA size, particle complex size, zeta potential, and vector material.

Previous studies have shown size-dependent internalization of particles through clathrin- and caveolae-mediated endocytosis pathways (16). It was found that microspheres with diameters <200 nm are taken up predominantly via clathrin-mediated endocytosis and are processed along this pathway to the lysosomal compartment. In contrast, larger particles (500 nm) are internalized almost exclusively *via* the caveolae-dependent route and are never seen in the lysosomal compartment. Because lipoplexes and polyplexes in our study had almost the same particle size (CD = 103.2 ± 2.9 nm, PEI22 = 92.54 ± 11.13 nm, and PEI25 = 101.31 ± 2.17 nm) at their optimal ratios and sizes of pEGFP and $phVEGF_{165}$ at 4.7 kb and 4.75 kb, respectively, the size of the lipid/DNA complexes was not a determinant factor for gene transfection efficiency in this study. Additionally, high zeta potential is preferred for higher transfection efficiency; it seemed that the zeta potential did not significantly influence the outcome of transfection after reaching a threshold level in our current study. The PEI22-DNA had the lowest zeta potential (26.17 ± 1.3 mV) compared with CD-DNA (45.97 ± 1.02 mV) and PEI25-DNA (36.42 ± 1.15 mV) at their respective optimum ratios. However, the highest transfection efficiency was achieved by PEI22. This indicates that zeta potentials as low as 26.17 mV are sufficient for binding complexes with the cell surface (17).

In the current study, it was the pathway through which the transfectant/DNA complexes enter into the cell and nuclei that plays a significant role in gene transfection efficiency. Lipoplexes are taken up uniquely by clathrin-mediated endocytosis with subsequent destruction of endosomes within the cell (18). The endosomal membrane destabilization results from the intermingling of lamellar phase–perturbing lipids with the endosomal membrane. The presence of negatively charged lipid phosphatidylserine may amplify destabilization of bilayer membrane organization upon its interaction with the cationic lipid, simultaneously causing competitive dissociation of DNA from the lipoplex and its subsequent release into the cytosol (19). Polyplexes

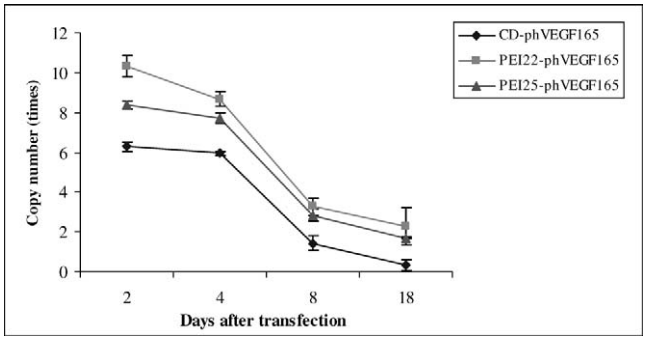

Figure 8. QRT-PCR for $hVEGF_{165}$ expression from CD-$phVEGF_{165}$-, PEI22-$phVEGF_{165}$-, and PEI25-$phVEGF_{165}$-transfected hSkMs as a function of time.

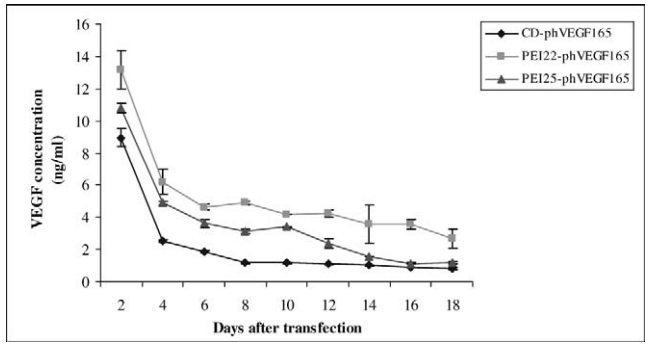

Figure 9. ELISA for $hVEGF_{165}$ protein secreted from CD-$phVEGF_{165}$-, PEI22-$phVEGF_{165}$-, and PEI25-$phVEGF_{165}$-transfected hSkMs as a function of time.

are taken up by clathrin- and caveolae-mediated endocytosis. However, only the caveolae-mediated route leads to efficient transfection. It has been proposed that polyplex DNA is released from the endosomal compartment as a result of osmotic bursting of the endosomes caused by an excessive influx of protons (20). Thus, the lower transfection efficiency by CD lipoplexes compared with PEI polyplexes for hSkMs was anticipated. The better transfection efficiency of PEI22 than PEI25 is due to the fact that PEI25 polyplexes can only translocate plasmid DNA into nuclei dominantly during the S/G_2 phase of the cell cycle, whereas PEI22 polyplexes can translocate plasmid DNA into nuclei independent of the cell cycle (12, 14, 15).

Based on the optimized transfection conditions, primary hSkMs were transfected with CD and PEI carrying $phVEGF_{165}$ for therapeutic angiogenesis. The transfected hSkMs efficiently expressed $hVEGF_{165}$ after transfection with the three types of complexes as demonstrated by fluorescent immunostaining. The expression of $hVEGF_{165}$ mRNA was significantly upregulated after transfection. The amount of protein secreted by hSkMs transfected with CD-$phVEGF_{165}$, PEI22-$phVEFG_{165}$, and PEI25-$phVEGF_{165}$ was as high as 6.96 ng/ml, 13.2 ng/ml, and 10.8 ng/ml, respectively, 2 days after transfection. These levels were sufficient to induce neovascularization, similar to another study which reported that rat skeletal myoblasts expressing 2.78 ± 0.2 ng/ml $hVEGF_{165}$ protein efficiently initiated neovascularization (21). Nonpathogenic adenoviral-associated vectors have been reported to deliver VEGF to achieve long-term sustained expression of VEGF (5). However, long-term constitutive expression of VEGF for therapeutic angiogenesis may be limited by the growth of abnormal blood vessels and hemangiomas. Transient, localized angiogenic protein delivery is preferred for therapeutic angiogenesis.

In conclusion, gene transfection efficiencies of CD liposome and PEI22 and PEI25 polymer transfection into primary hSkMs was related to cell passage number with the earlier passaged cells showing better transgene uptake. Therefore, the transfection necessitates optimization of conditions when primary hSkMs are to be genetically modified using nonviral vectors to achieve the highest transfection efficiency with minimum cell damage. Trypsinization may further improve gene transfection efficiency. CD liposome– and PEI22 and PEI25 polymer– mediated angiogenic gene transfection with hSkMs is feasible and could be a potential strategy for treatment of ischemic disease for angiomyogenesis.

1. Ye L, Haider HKh, Sim EKW. Adult stem cells for cardiac repair: a choice between skeletal myoblasts and bone marrow stem cells. Exp Biol Med (Maywood) 231:8–19, 2006.
2. Ye L, Haider HKh, Jiang SJ, Sim EKW. Therapeutic angiogenesis: devising new strategies based on past experiences. Basic Res Cardiol 99:121–132, 2004.
3. Haider HKh, Ye L, Jiang SJ, Ge RW, Law PK, Chua T, Wong P, Sim EKW. Angiomyogenesis for cardiac repair using human myoblasts as carriers of human vascular endothelial growth factor. J Mol Med 82: 539–549, 2004.
4. Ye L, Haider KhH, Jiang SJ, Ling LH, Ge RW, Law PK, Sim EKW. Reversal of myocardial injury using genetically modulated human skeletal myoblasts in a rodent cryoinjured heart model. Eur J Heart Fail 7:945–952, 2005.
5. Su H, Lu R, Kan YW. Adeno-associated viral vector-mediated vascular endothelial growth factor gene transfer induces neovascular formation in ischemic heart. Proc Natl Acad Sci U S A 97:13801–13806, 2000.
6. Lee RJ, Springer ML, Blanco-Bose WE, Shaw R, Ursell PC, Blau HM. VEGF gene delivery to myocardium: deleterious effects of unregulated expression. Circulation 102:898–901, 2000.
7. Lehrman S. Virus treatment questioned after gene therapy death. Nature 401:517–518, 1999.
8. Liu Q, Muruve DA. Molecular basis of the inflammatory response to adenovirus vectors. Gene Ther 10:935–940, 2003.
9. Marshall E. Gene therapy death prompts review of adenovirus vector. Science 286:2244–2245, 2000.
10. Sun JY, Anand-Jawa V, Chatterjee S, Wong KK. Immune responses to adeno-associated virus and its recombinant vectors. Gene Ther 10:964–976, 2000.
11. Davis ME. Non-viral gene delivery systems. Biotechnology 13:128–131, 2002.
12. Lungwitz U, Breunig M, Blunk T, Göpferich A. Polyethylenimine-based non-viral gene delivery systems. Eur J Pharm Biopharm 60:247–266, 2005.
13. Campeau P, Chapdelaine P, Seigneurin-Venin S, Massie B, Tremblay JP. Transfection of large plasmids in primary human myoblasts. Gene Ther 8:1387–1394, 2001.
14. Brunner S, Sauer T, Carotta S, Cotton M, Saltik M, Wagner E. Cell cycle dependence of gene transfer by lipoplex, polyplex and recombinant adenovirus. Gene Ther 7:401–407, 2000.
15. Brunner S, Furtbauer E, Sauer T, Kursa M, Wagner E. Overcoming the nuclear barrier: cell cycle independent non-viral gene transfer with linear polyethylenimine or electroporation. Mol Ther 5:80–86, 2002.
16. Rejman J, Oberle V, Zuhorn IS, Hoekstra D. Size-dependent internalization of particles via the pathways of clathrin- and caveolae-mediated endocytosis. Biochem J 377:159–169, 2004.
17. Gautam A, Densmore CL, Xu B, Waldrep JC. Enhanced gene expression in mouse lung after PEI-DNA aerosol delivery. Mol Ther 2:63–70, 2000.
18. Rejman J, Conese M, Hoekstra D. Gene transfer by means of lipo- and polyplexes: role of clathrin and caveolae-mediated endocytosis. J Liposome Res 16:237–247; 2006.
19. Xu Y, Szoka FC Jr. Mechanism of DNA release from cationic liposome/DNA complexes used in cell transfection. Biochemistry 35: 5616–5623, 1996.
20. Boussif O, Lezoualc'h F, Zanta MA, Mergny MD, Scherman D, Demeneix B, Behr JP. A versatile vector for gene and oligonucleotide transfer into cells in culture and in vivo: polyethylenimine. Proc Natl Acad Sci U S A 92:7297–7301, 1995.
21. Suzuki K, Murtuza B, Smolenski RT, Sammut IA, Suzuki N, Kaneda Y, Yacoub MH. Cell transplantation for the treatment of acute myocardial infarction using vascular endothelial growth factor-expressing skeletal myoblasts. Circulation 104:I207-I212, 2001.